



**ICQM**

International Center  
for Quantum Materials



# Identify two CDW amplitude modes with extremely small energy scales in LaAgSb<sub>2</sub> by ultrafast pump-probe measurement

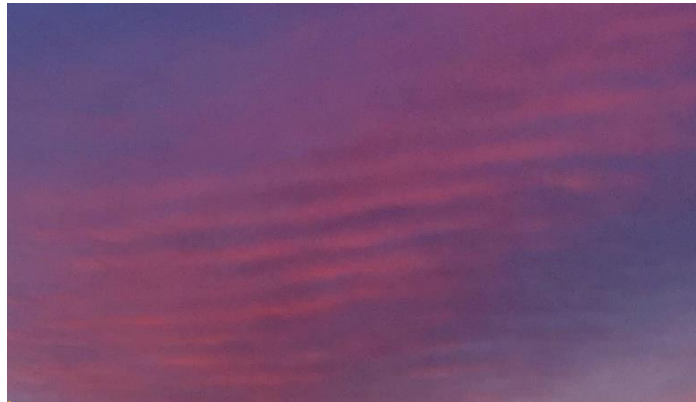
Nan-Lin Wang



**Collaborators:**

**R. Y. Chen**, S. J. Zhang, M. Y. Zhang, T. Dong

**ICQM, School of Physics,  
Peking University, Beijing, China**



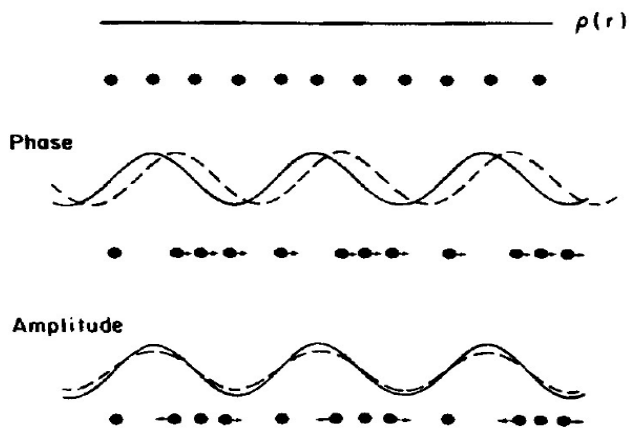
Density modulation



# About CDW condensate:

**Single particle excitation:** an energy gap;

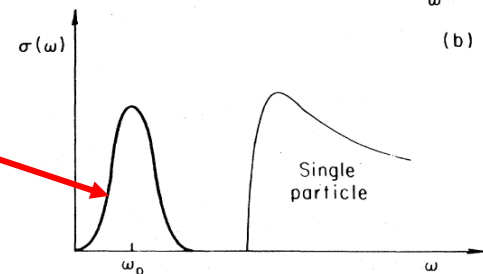
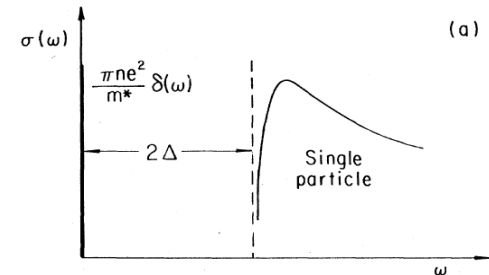
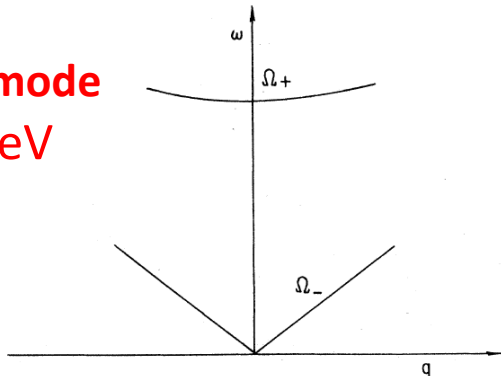
**Collective excitations:** amplitude and phase modes.



**Phase excitation** corresponds to the translational motion of the undistorted condensate

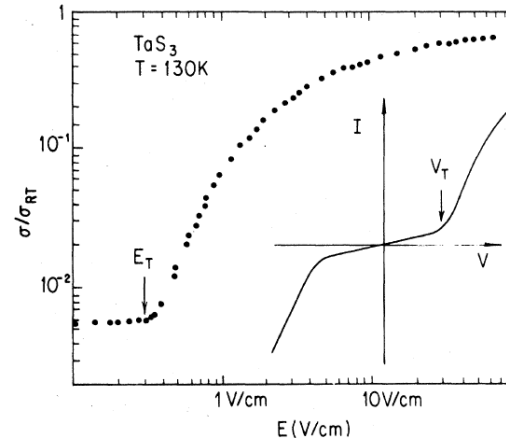
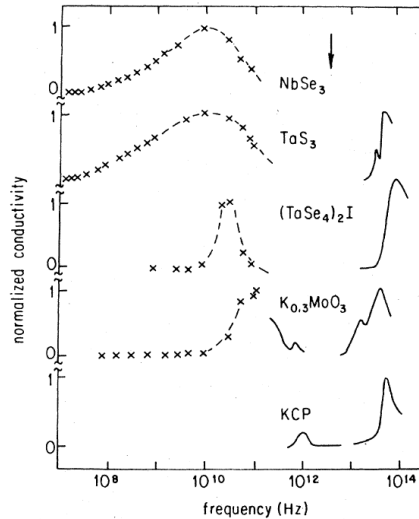
$\omega_\phi(q=0) = 0$ . because no change in condensation energy

**amplitude mode gap**  $\sim 10$  meV



Pinning by impurities

The pinning/depinning of phase mode has dramatic effect on charge transport properties. By applying dc electric field, the phase mode can be driven into a current-carrying state, leading to nonlinear current-voltage characteristics.



G. Gruner,  
RMP (1988)

However, effect of amplitude mode (Raman active) on the physical properties was much less studied.

Here we show that a layered CDW compound LaAgSb<sub>2</sub> has unusually small energy scales of the amplitude modes.

# Outline

- Introduction about the material

Two CDW orders in LaAgSb<sub>2</sub> with very small  $2\mathbf{K}_F$

- Optical spectroscopy data

CDW energy gaps

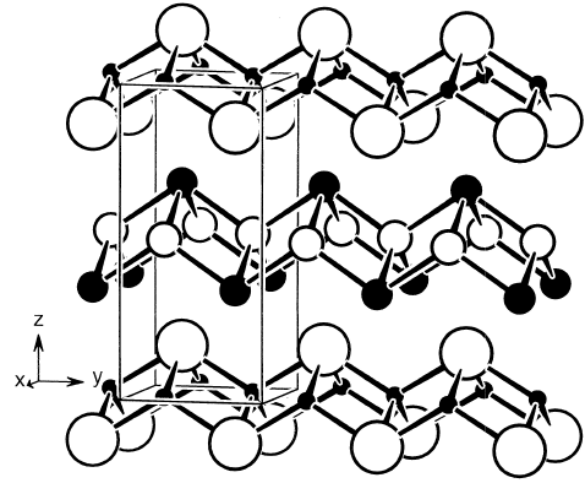
- Ultrafast pump-probe measurement

**Key result: Identify two CDW amplitude modes with extremely small energy scales**

- Summary

# About the material

LaAgSb<sub>2</sub> has ZrCuSi<sub>2</sub> structure



- **First report of quaternary silicide arsenide ZrCuSiAs structure**

V. Johnson and W. Jeitschko, J. Solid State Chem. 11, 161 (1974)

- **First ternary compound with similar structure ZrCuSi<sub>2</sub>**

H. Sprenger, J. Less-Common Met. 34, 39 (1974)

- **Related compounds followed:**

HfCuSi<sub>2</sub> (1975), CaMnBi<sub>2</sub> (1980), UCuAs<sub>2</sub> (1987),

# Ternary Arsenides $ACuAs_2$ and Ternary Antimonides $A\text{AgSb}_2$ ( $A =$ Rare-Earth Elements and Uranium) with $HfCuSi_2$ -Type Structure

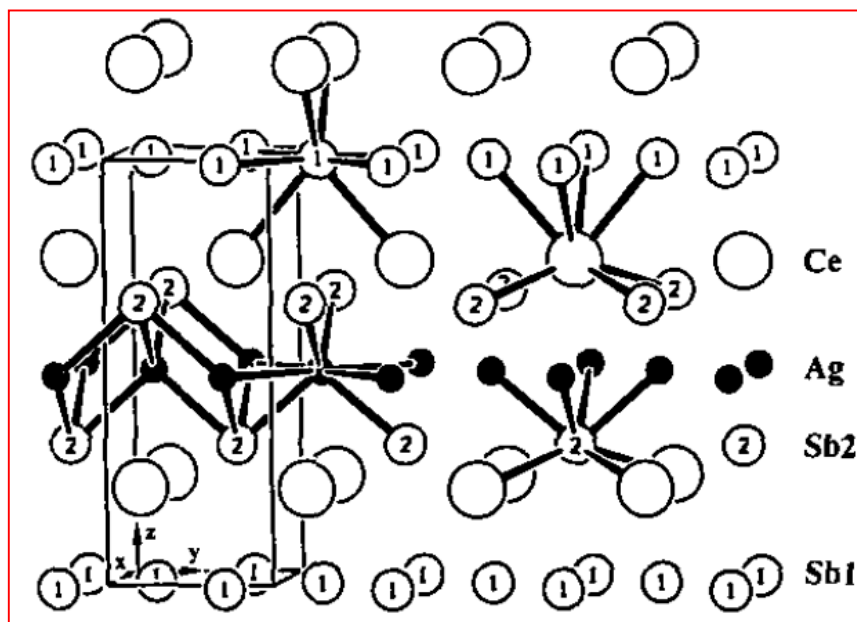
Markus Brylak, Manfred H. Möller, and Wolfgang Jeitschko

*Anorganisch-Chemisches Institut der Universität Münster, Wilhelm-Klemm-Strasse 8, D-48149 Münster, Germany*

Received May 13, 1994; accepted July 15, 1994

Lattice Constants of Arsenides and Antimonides with the Tetragonal  $HfCuSi_2$ -Type Structure<sup>a</sup>

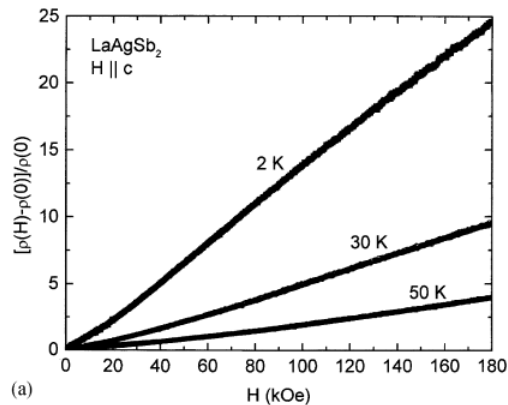
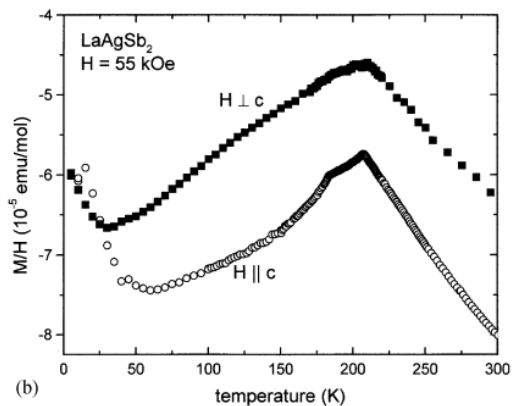
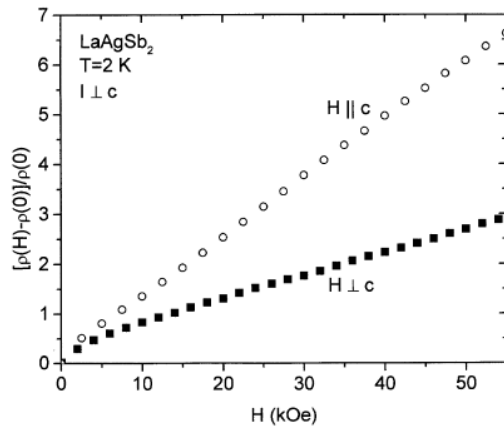
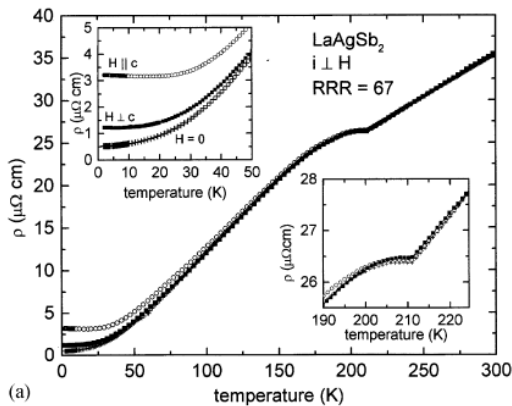
Compound	<i>a</i> (pm)	<i>c</i> (pm)	<i>c/a</i>	<i>V</i> (nm <sup>3</sup> )
YCuAs <sub>2</sub>	388.62(8)	987.10(3)	2.540	0.1491
LaCuAs <sub>2</sub>	404.8(3)	1027(1)	2.537	0.1683
CeCuAs <sub>2</sub>	401.81(7)	1010.4(2)	2.515	0.1631
PrCuAs <sub>2</sub>	399.42(8)	1006.8(3)	2.521	0.1606
NdCuAs <sub>2</sub>	396.7(1)	1005.5(5)	2.535	0.1582
SmCuAs <sub>2</sub>	393.50(6)	997.2(2)	2.534	0.1544
GdCuAs <sub>2</sub>	391.05(4)	992.9(2)	2.549	0.1518
TbCuAs <sub>2</sub>	389.42(4)	987.9(2)	2.537	0.1498
DyCuAs <sub>2</sub>	388.20(4)	984.8(2)	2.537	0.1484
HoCuAs <sub>2</sub>	387.24(9)	982.2(3)	2.536	0.1473
ErCuAs <sub>2</sub>	385.83(7)	978.9(3)	2.537	0.1457
TmCuAs <sub>2</sub>	384.87(7)	976.9(3)	2.538	0.1447
YbCuAs <sub>2</sub>	384.5(1)	974.5(5)	2.535	0.1441
LuCuAs <sub>2</sub>	383.42(7)	974.2(3)	2.541	0.1432
UCuAs <sub>2</sub> <sup>b</sup>	394.8(2)	953.3(5)	2.415	0.1486
YAgSb <sub>2</sub>	427.65(3)	1048.8(1)	2.452	0.1918
LaAgSb <sub>2</sub>	439.03(6)	1084.0(2)	2.469	0.2089
CeAgSb <sub>2</sub>	436.3(1)	1069.9(4)	2.452	0.2037
PrAgSb <sub>2</sub>	434.99(6)	1067.0(3)	2.453	0.2019
NdAgSb <sub>2</sub>	433.53(3)	1063.0(2)	2.452	0.1998
SmAgSb <sub>2</sub>	431.2(1)	1055.5(5)	2.448	0.1962
GdAgSb <sub>2</sub>	429.52(7)	1050.6(2)	2.446	0.1938
TbAgSb <sub>2</sub>	428.33(7)	1047.6(2)	2.446	0.1922
DyAgSb <sub>2</sub>	427.43(5)	1044.2(3)	2.443	0.1908
HoAgSb <sub>2</sub>	426.62(9)	1042.2(3)	2.443	0.1897
ErAgSb <sub>2</sub>	425.65(8)	1039.0(3)	2.441	0.1883
TmAgSb <sub>2</sub>	425.29(7)	1039.0(3)	2.443	0.1880
UAgSb <sub>2</sub>	432.40(6)	1031.8(2)	2.386	0.1929



# Basic properties

*K.D. Myers et al. / Journal of Magnetism and Magnetic Materials 205 (1999) 27–52*

## LaAgSb<sub>2</sub>



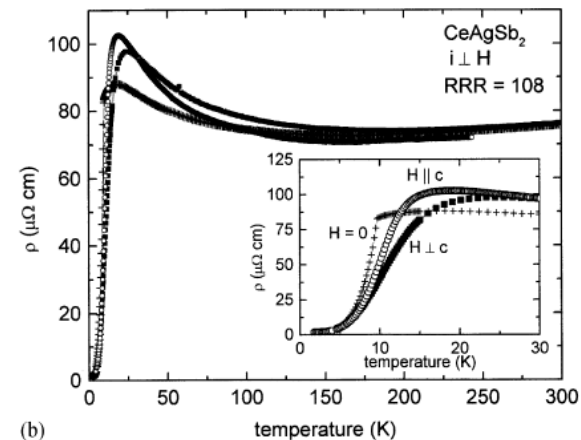
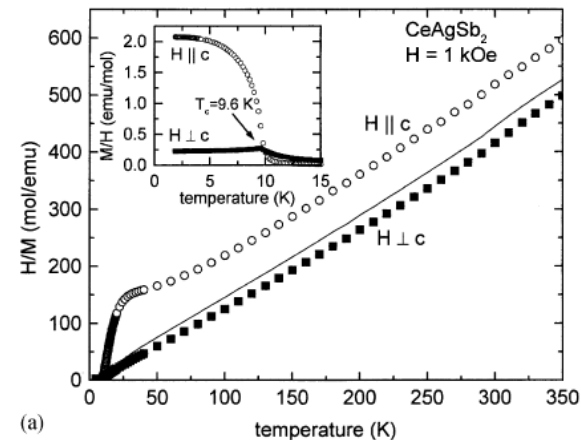
Two phase transitions

CDW or SDW speculated

Linear MR

Dirac fermion?

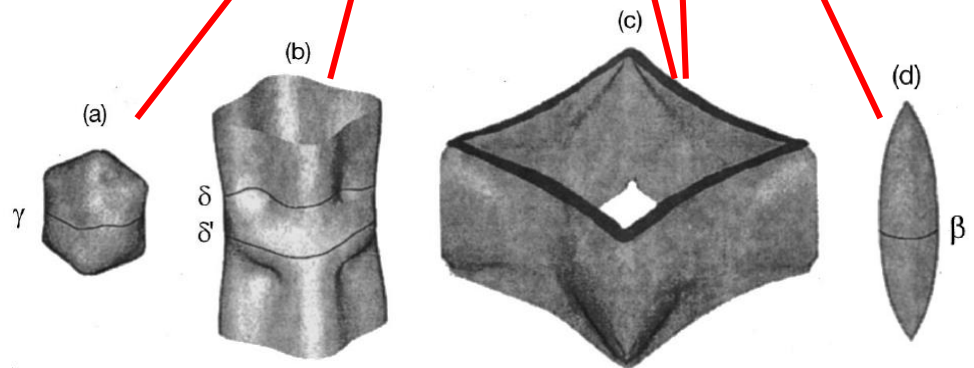
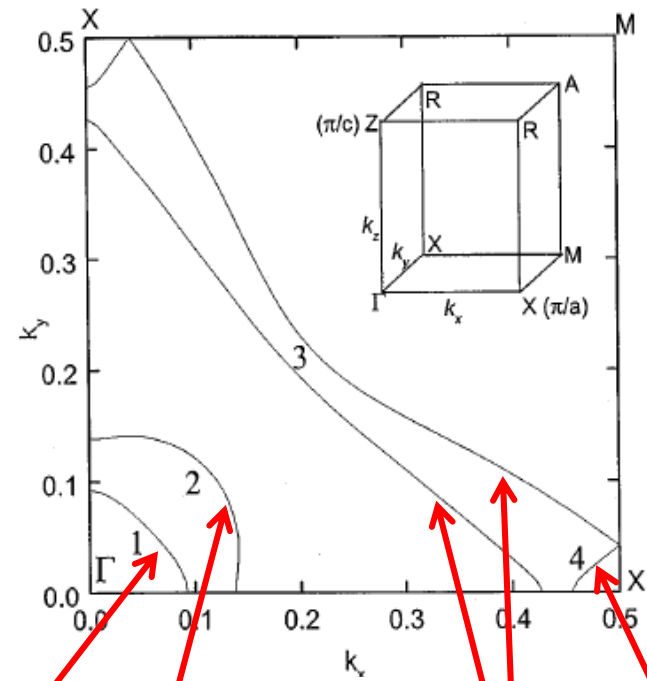
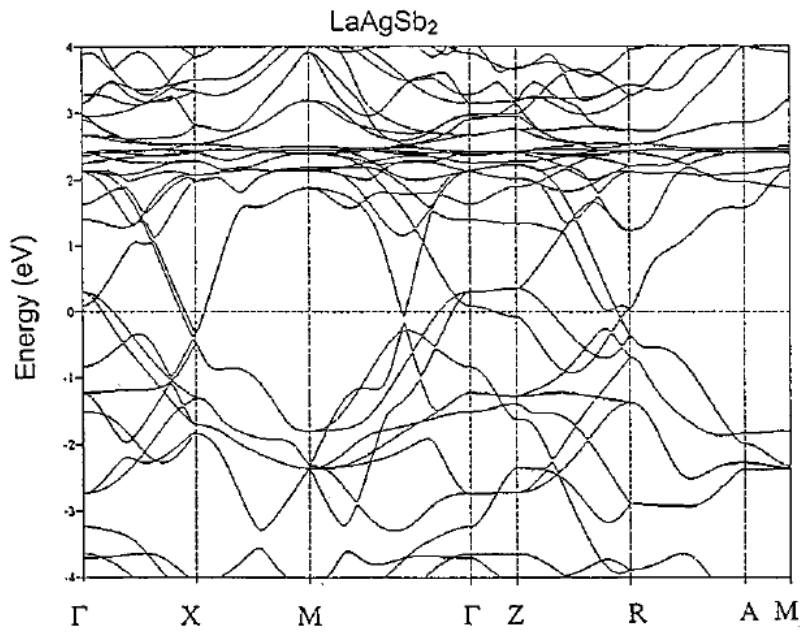
## CeAgSb<sub>2</sub>



Heavy fermions



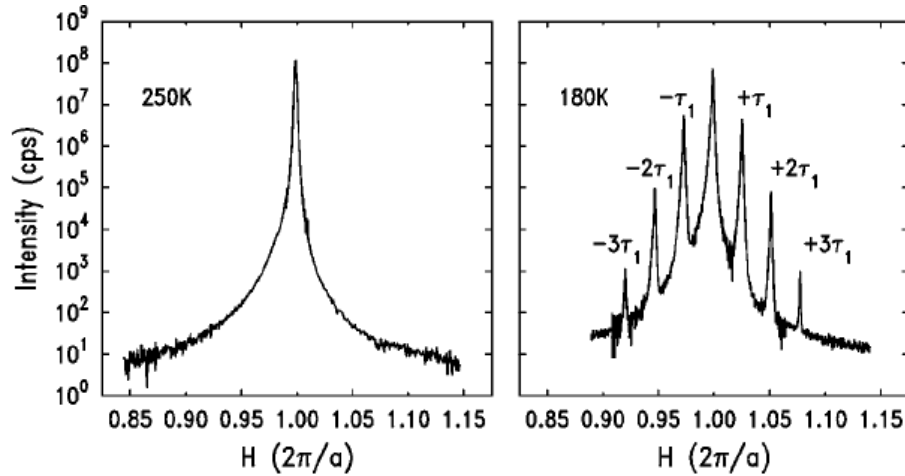
# LDA band structures



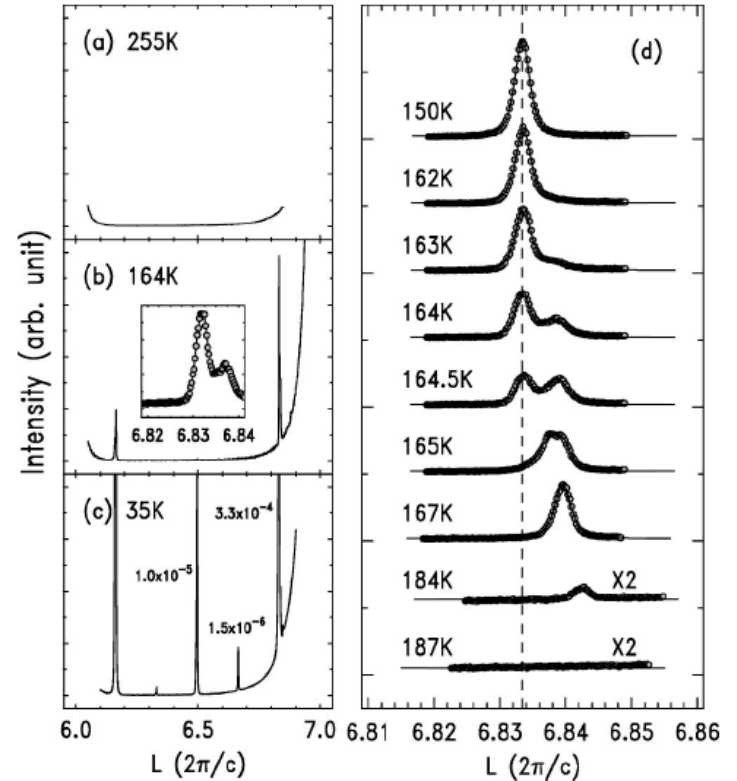
K. D. Myers et al., PRB 60, 13731 (1999)

# Synchrotron X-ray diffraction

C. Song et al. PRB 68, 035113 (2003)



Along (0 0 1) direction



Along (0 0 1) direction  
around (1 0 7) peak

$$T_{1,CDW} = 207 \text{ K,}$$

$$\tau_1 \sim 0.026(2\pi/a)$$

$$2\pi/\tau_1 \sim 40a$$

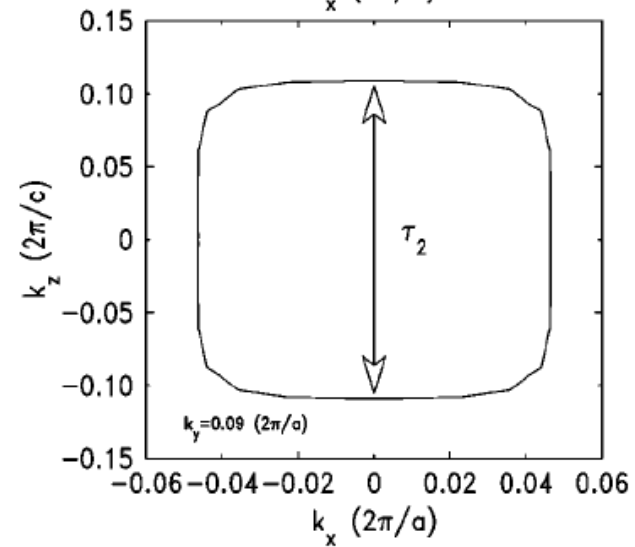
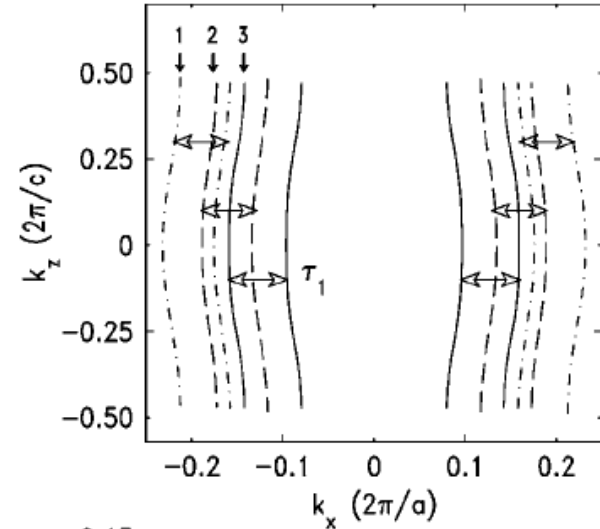
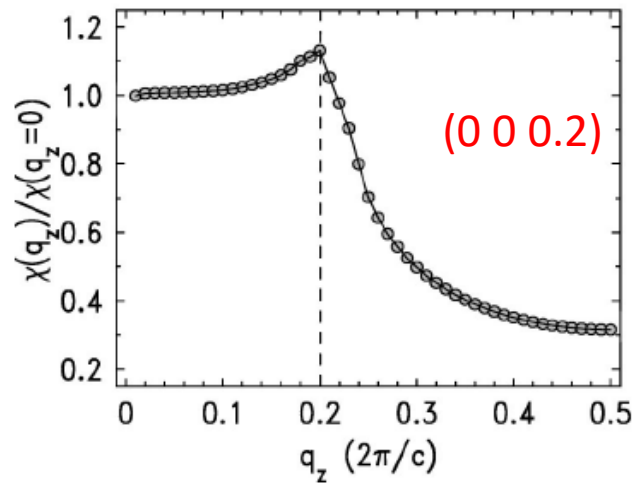
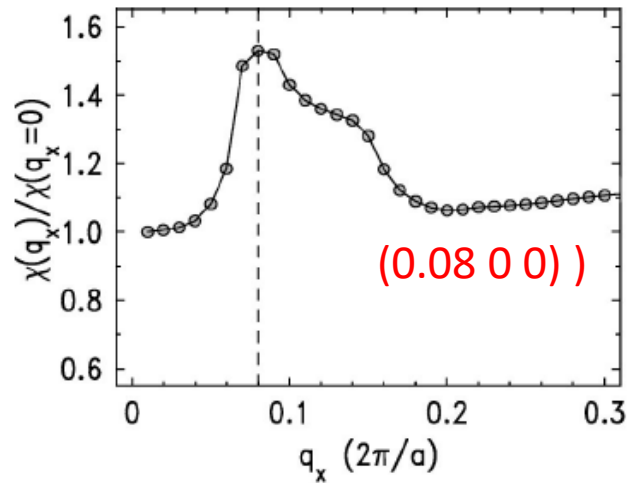
a periodic charge and  
lattice modulation

$$T_{2,CDW} = 186 \text{ K}$$

$$\tau_2 \sim 0.16(2\pi/c)$$

(0.026 0 0) of  $\tau_1$ -CDW

(0 0 0.166) of  $\tau_2$ -CDW.



Generalized susceptibility

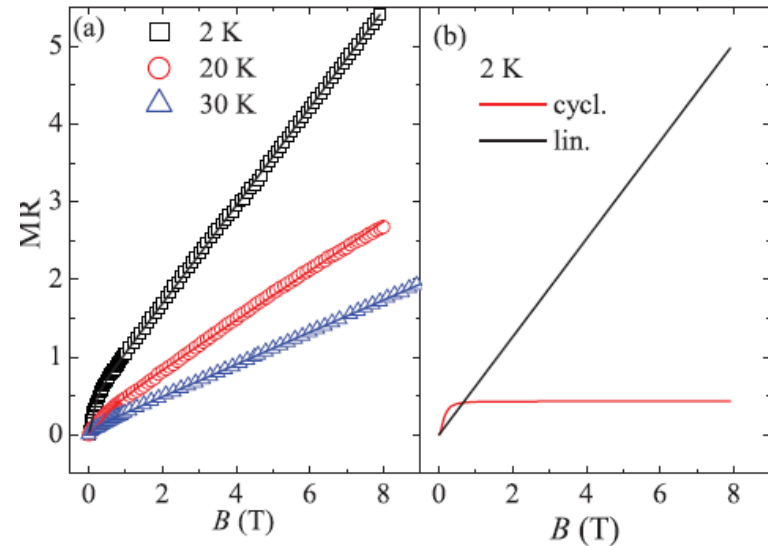
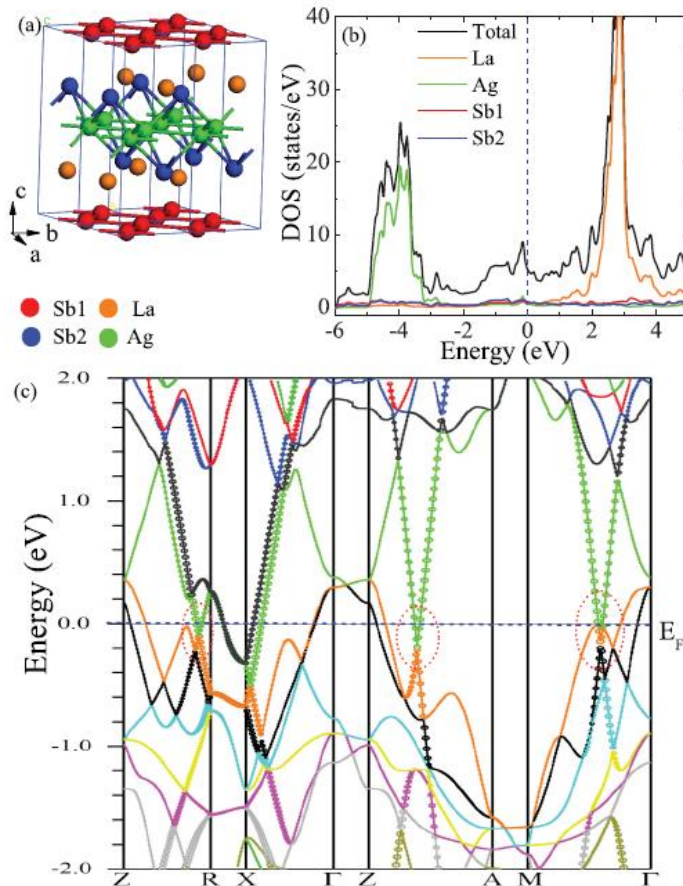
C. Song et al. PRB 68, 035113 (2003)

## Multiband effects and possible Dirac states in LaAgSb<sub>2</sub>

Kefeng Wang (王克锋) and C. Petrovic

*Condensed Matter Physics and Materials Science Department, Brookhaven National Laboratory, Upton, New York 11973, USA*

(Received 13 July 2012; revised manuscript received 4 September 2012; published 25 October 2012)



$$\text{MR} = \frac{1}{2\pi} \left( \frac{e^2}{\epsilon_\infty \hbar v_F} \right)^2 \frac{N_i}{en^2} B \ln(\epsilon_\infty),$$

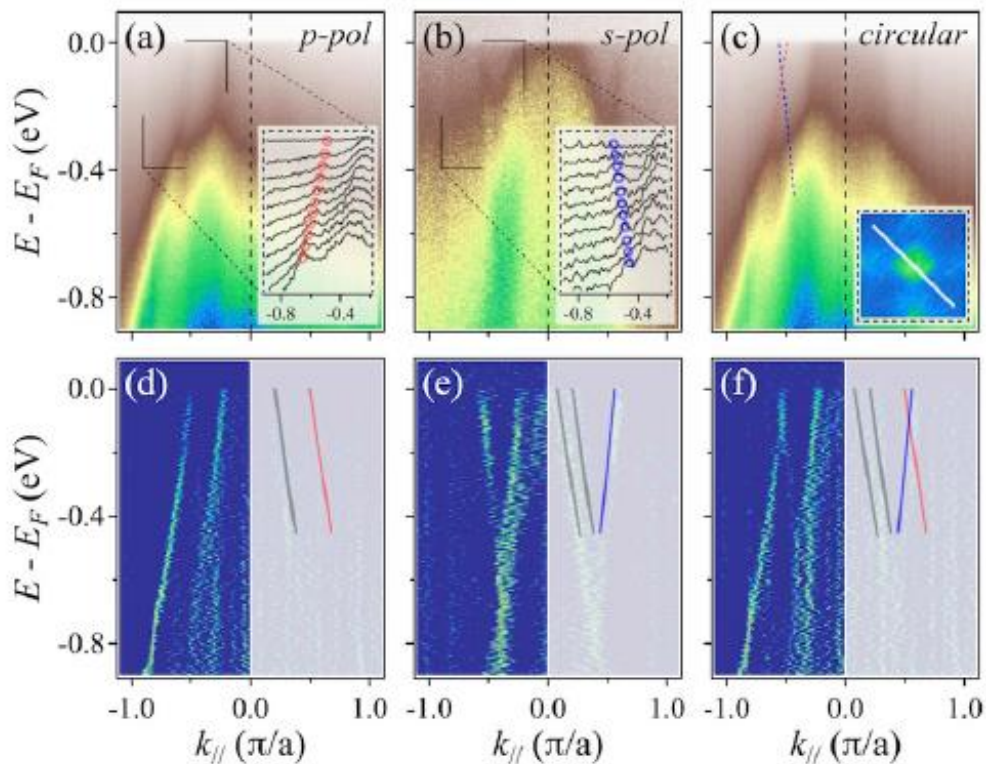
$$B^* = \frac{1}{2e\hbar v_F^2} (E_F + k_B T)^2$$

$$v_F \sim 1.46 \times 10^5 \text{ ms}^{-1}$$

Linear MR could arise due to the quantum limit of Dirac fermions in the high magnetic field.

## Observation of Dirac-like band dispersion in LaAgSb<sub>2</sub>

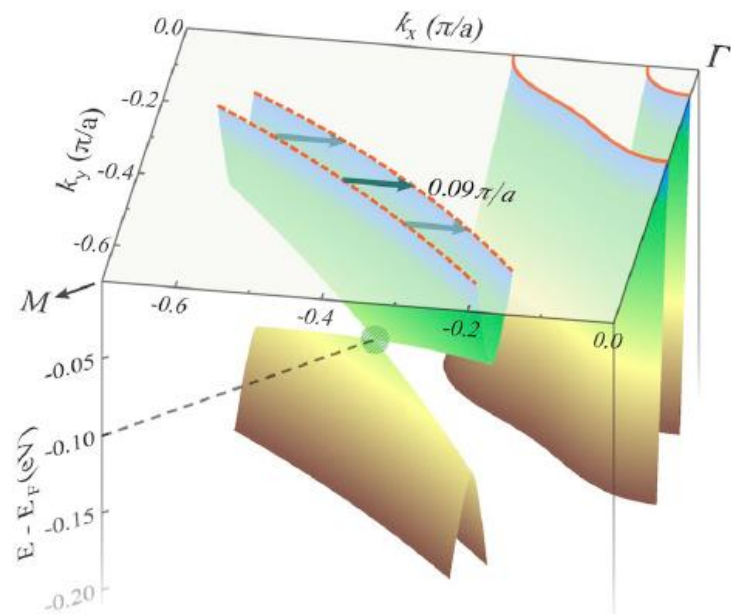
X. Shi,<sup>1</sup> P. Richard,<sup>1,2,\*</sup> Kefeng Wang,<sup>3,†</sup> M. Liu,<sup>1</sup> C. E. Matt,<sup>4,5</sup> N. Xu,<sup>4,6</sup> R. S. Dhaka,<sup>4,6,7</sup> Z. Ristic,<sup>4,6,8</sup> T. Qian,<sup>1</sup>  
 Y.-F. Yang,<sup>1,2</sup> C. Petrovic,<sup>3</sup> M. Shi,<sup>4</sup> and H. Ding<sup>1,2,‡</sup>



Dirac point locates 100 meV below  $E_F$

$$V_{F1} = 5.7 \times 10^5 \text{ m/s}$$

$$V_{F2} = 8 \times 10^5 \text{ m/s}$$



Nesting wave vector  $0.09\pi/a$

**The relationship between Dirac fermions and CDW?**

# Single crystal growth and characterizations

- We grew LaAsSb<sub>2</sub> single crystal by Sb flux method.

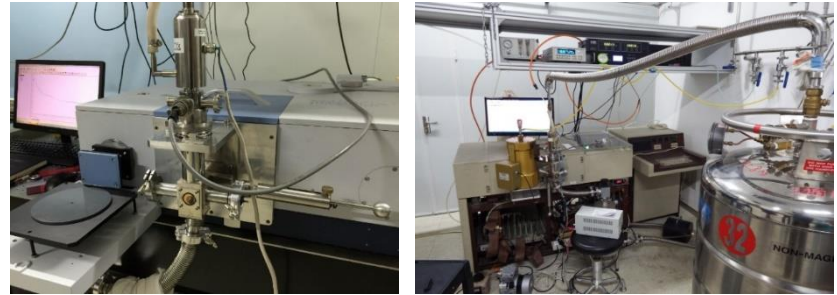
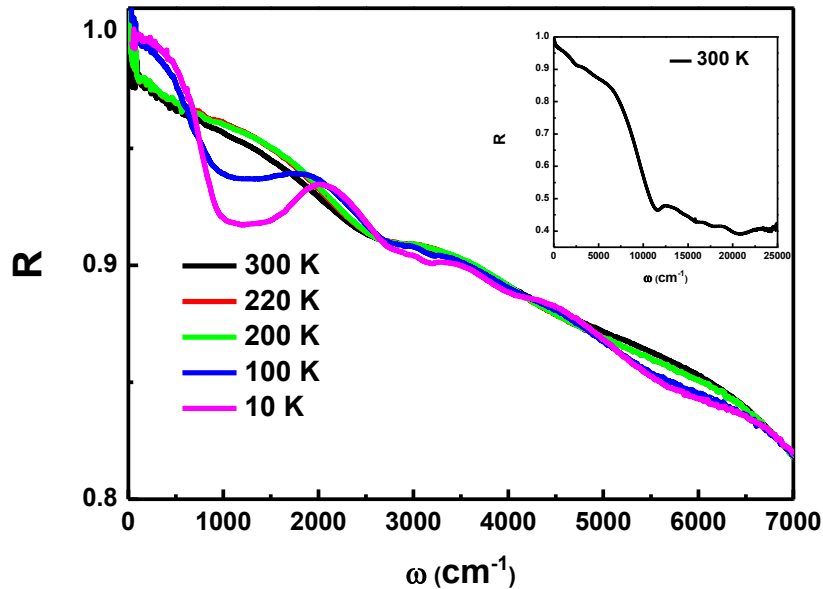


- The crystals were characterized by XRD, EDX,  $\rho(T)$ ,  $\chi(T)$ .
- Optical spectroscopy
- Pump-probe measurement



# Optical spectroscopy measurement

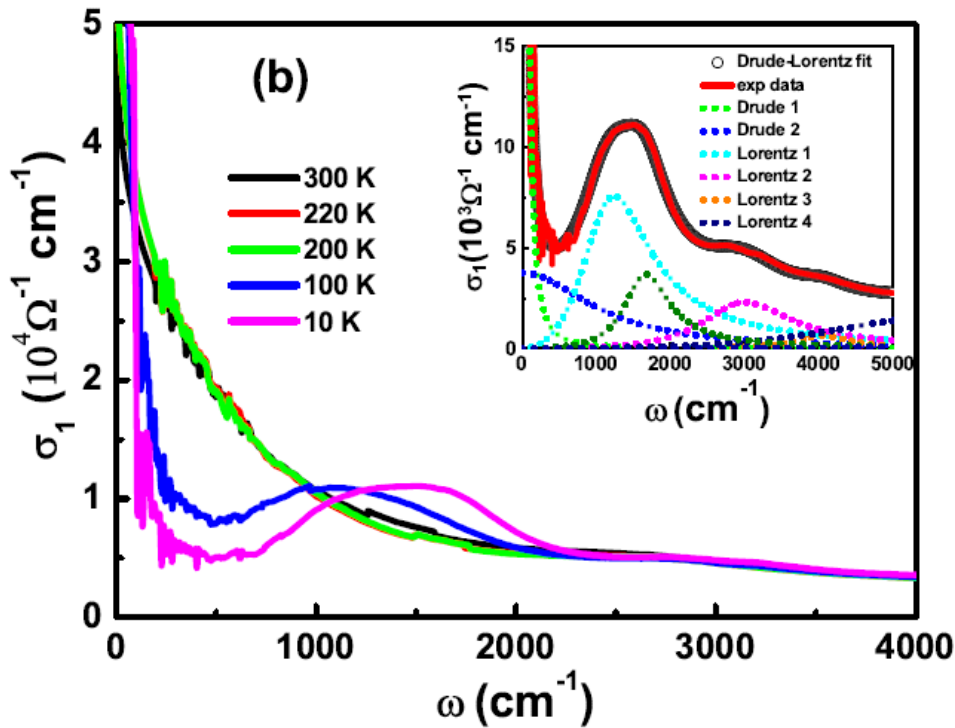
We measured  $R(\omega)$  (30-25000  $\text{cm}^{-1}$ ) using Bruker 80 v and 113 v spectrometers



In-situ gold- or aluminum-deposit technique

$$R(\omega) \xrightarrow{KK} \theta(\omega) \rightarrow \begin{cases} n(\omega), \kappa(\omega) \\ \varepsilon_1(\omega), \varepsilon_2(\omega) \\ \sigma_1(\omega), \sigma_2(\omega) \end{cases}$$

$$\theta(\omega) = -\frac{\omega}{\pi} \int_0^{\infty} \frac{\ln R(\omega') - \ln R(\omega)}{\omega'^2 - \omega^2} d\omega'$$



- ✓ Observation of partial CDW gaps:  $\Delta_1 \approx 207 \text{ meV}; \Delta_2 \approx 154 \text{ meV}$
- ✓ Most part of the free carrier spectral weight was removed due to the opening of CDW gaps.  $\omega_p = 40400 \text{ cm}^{-1}$  at 300 K to  $25500 \text{ cm}^{-1}$  at 10 K.

the Drude-Lorentz model to fit the optical conductivity,

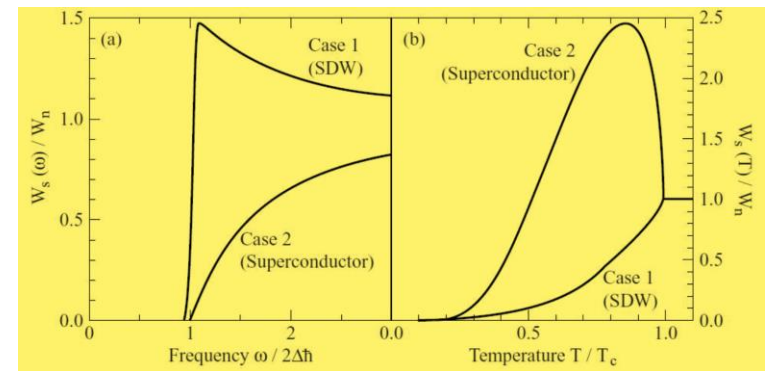
$$\epsilon(\omega) = \epsilon_\infty - \sum_s \frac{\omega_{ps}^2}{\omega^2 + i\omega/\tau_{Ds}} + \sum_j \frac{S_j^2}{\omega_j^2 - \omega^2 - i\omega/\tau_j}$$

**Energy gaps for symmetry broken states: Coherence factors**

$$\alpha_s = \int |M|^2 F(\Delta, E, E + \hbar\omega) N_s(E) N_s(E + \hbar\omega) [f(E) - f(E + \hbar\omega)] dE$$

$$F(\Delta, E, E') = \frac{1}{2} \left( 1 + \eta \frac{\Delta^2}{EE'} \right)$$

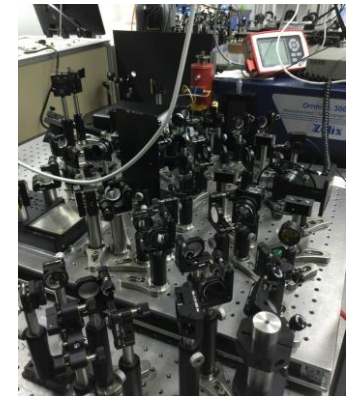
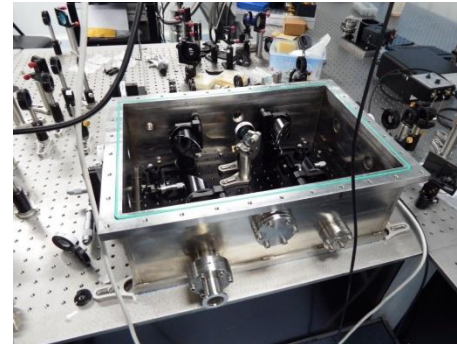
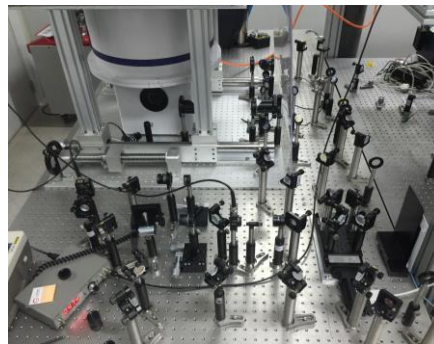
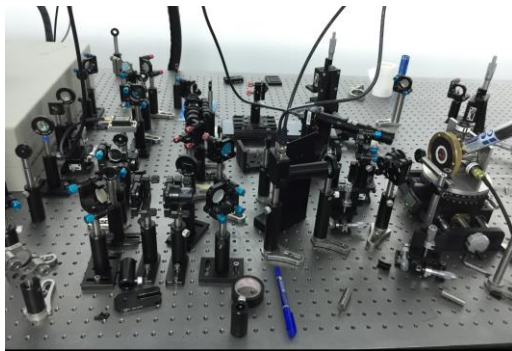
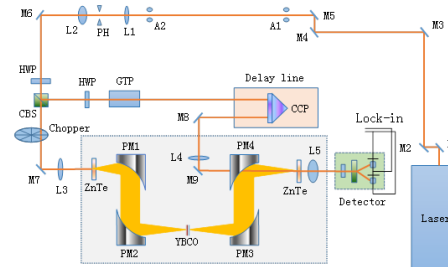
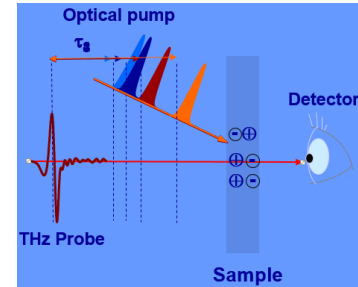
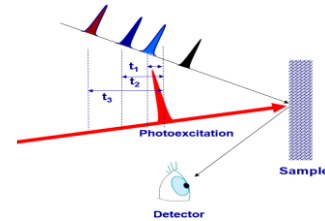
$$\eta = \begin{cases} -1 & \text{case I} \\ +1 & \text{case II} \end{cases}$$





# Efforts on time-resolved optical systems

- Pump-probe with 80 MHz repetition rate
- Pump-probe with 1 KHz repetition rate
- Time domain terahertz spectroscopy
- Optical pump- THz probe
- THz pump- THz probe
- Mid-infrared pump –THz probe



# The transient photo-induced reflectivity $\Delta R/R$ as a function of time delay at different temperatures.

Ti:sapphire oscillator: 800 nm, pulse width 100 fs, repetition rate 80 MHz  
Pump fluence is  $1 \sim 2 \mu\text{J}/\text{cm}^2$

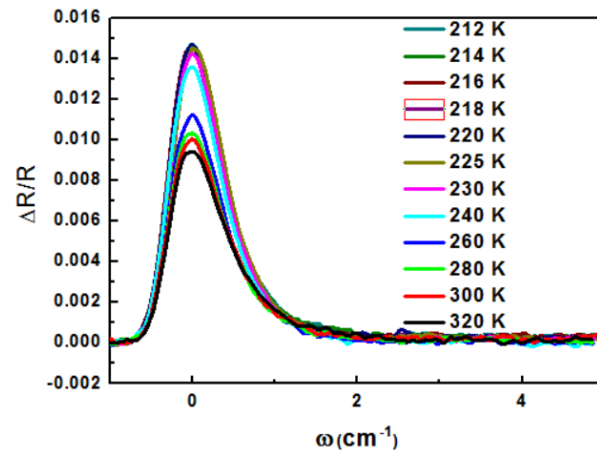
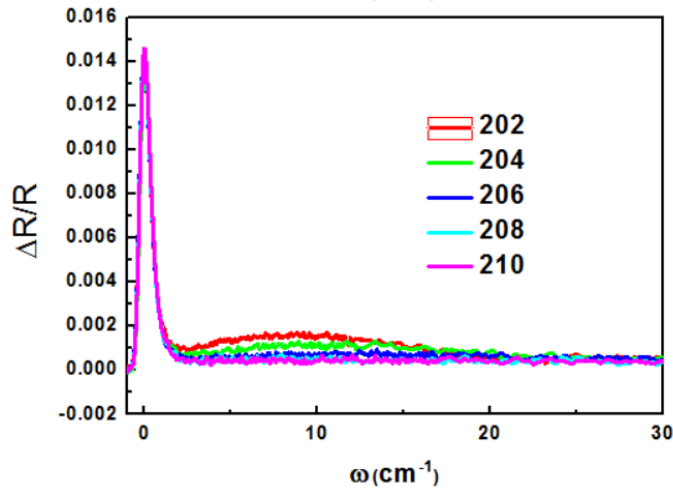
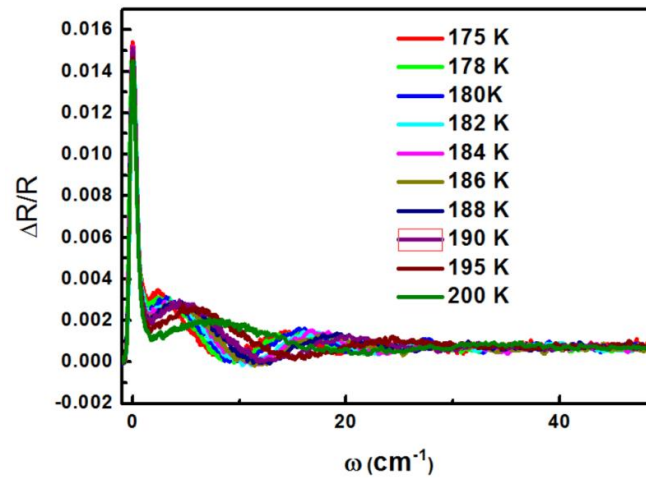
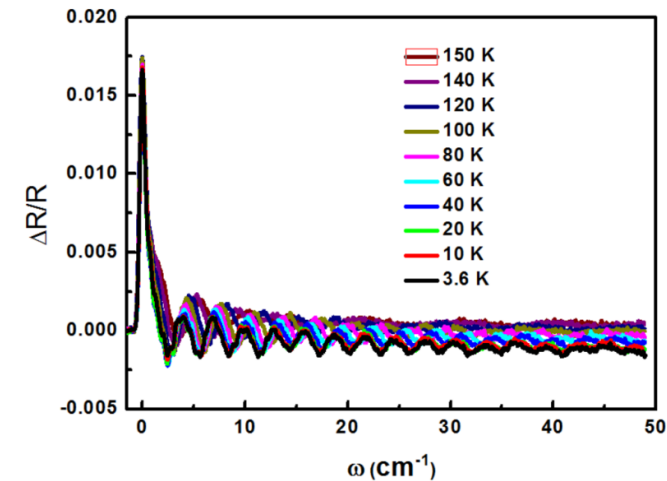
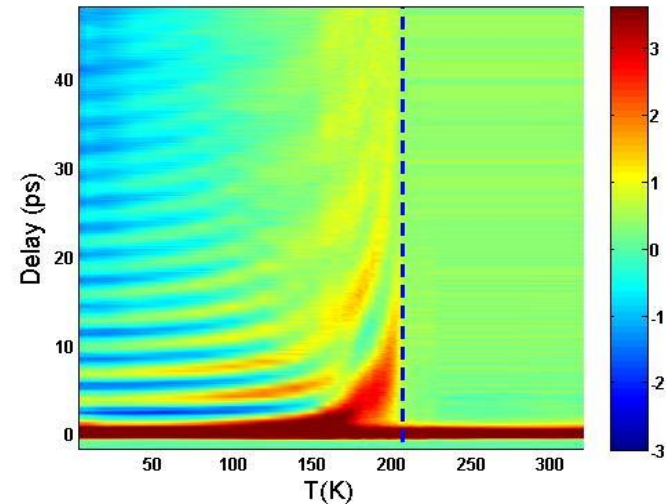
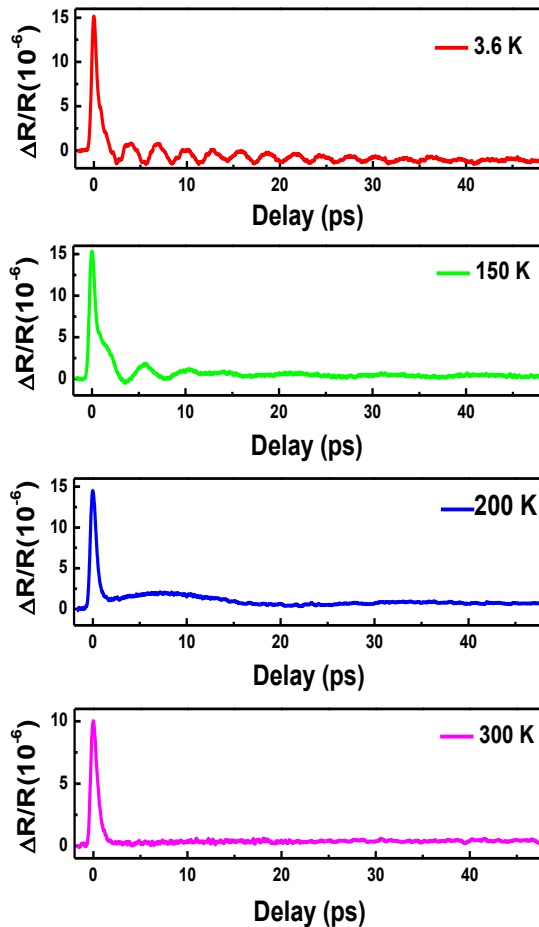
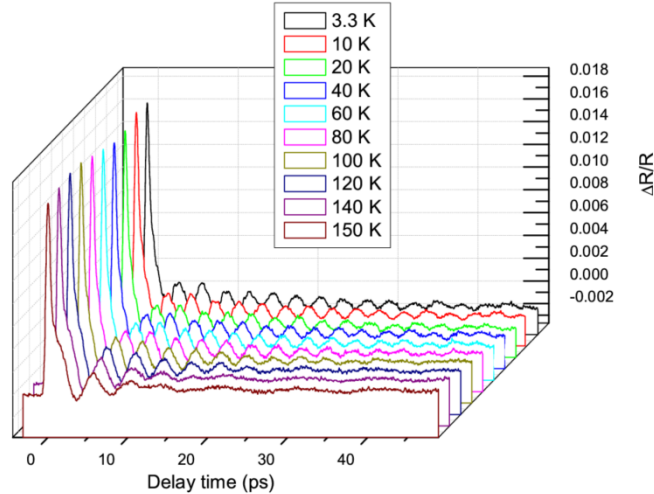


# Photo-induced reflectivity

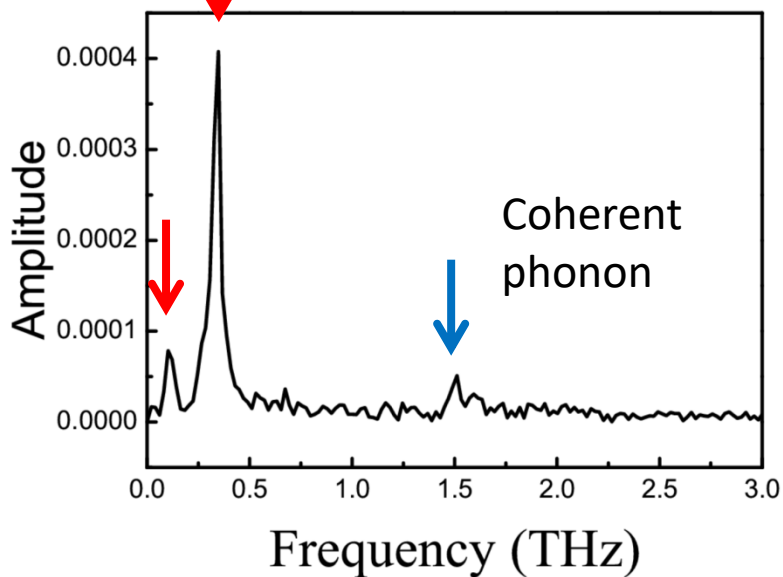


- $\Delta R/R = A \exp(-t/\tau) + C$  at high temperatures.
- **Emergence of strong oscillations upon entering the CDW states.**
- The amplitude  $A$  and relaxation time  $\tau$  are almost constant across the two CDW transition temperatures.

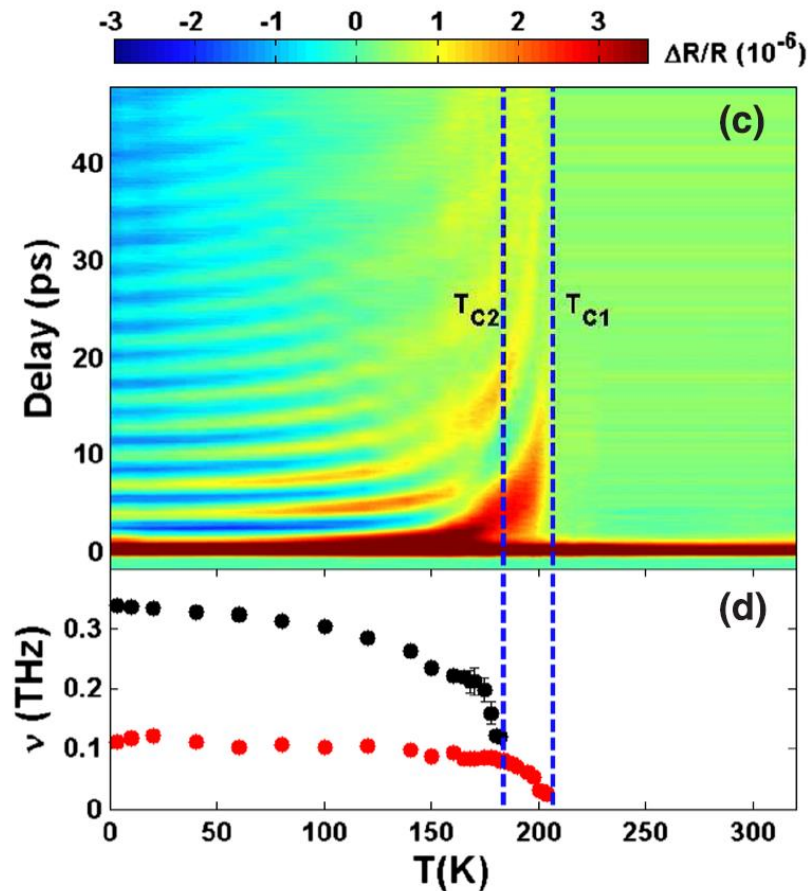


amplitude  
modes

Fourier Transformation

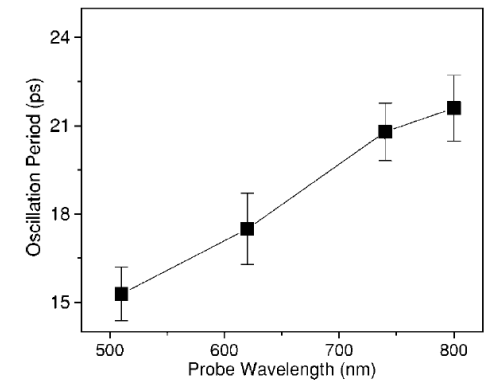
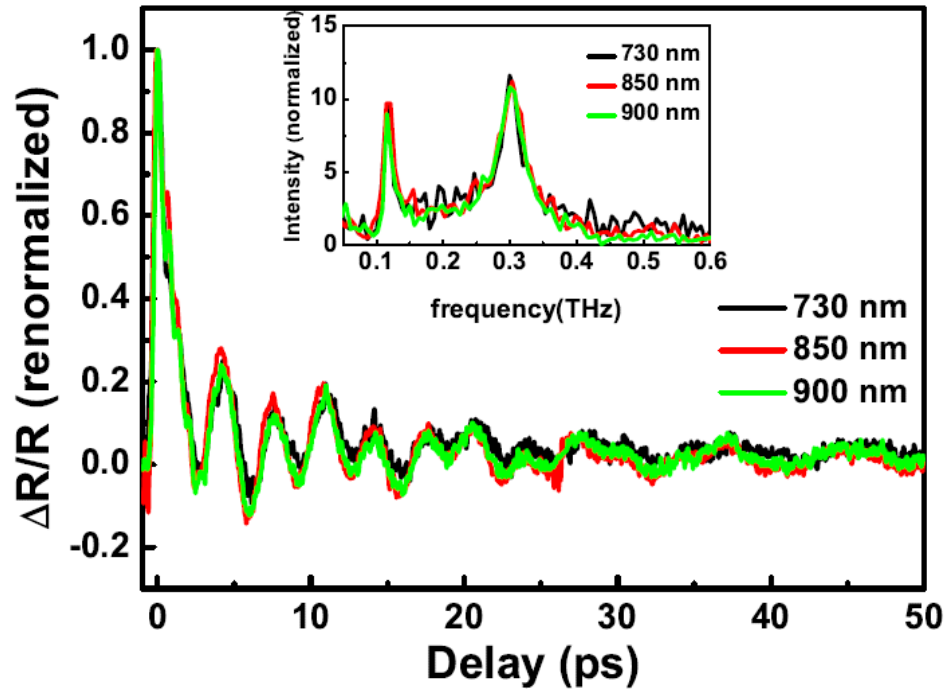


Extremely low energy scale  
of amplitude modes

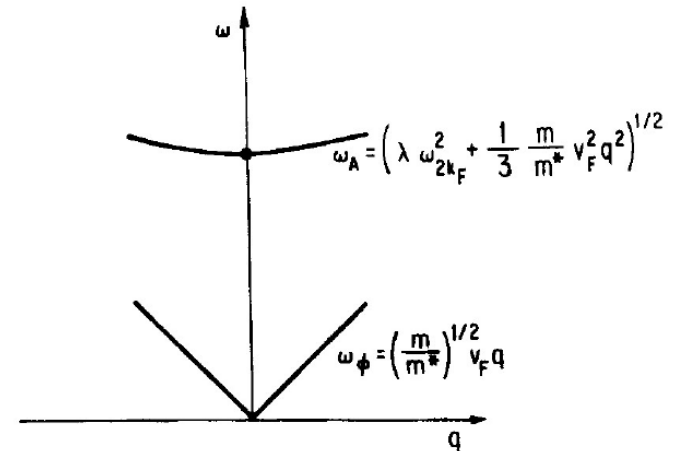
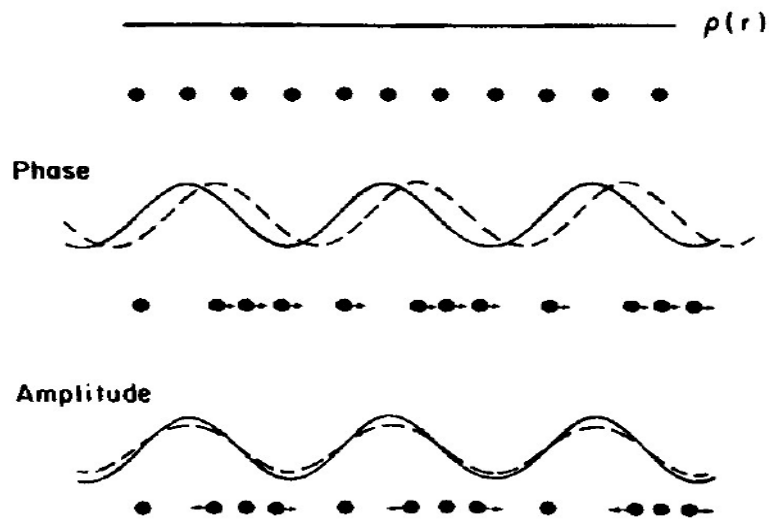


$\nu_1=0.12$  THz (4  $\text{cm}^{-1}$ ), corresponds to the  
higher CDW phase transition.  
 $\nu_2=0.34$  THz (11  $\text{cm}^{-1}$ ), corresponds to the  
lower CDW phase transition.

Coherent acoustic phonons can be excluded, because no energy shift was observed when the wave length of probe beam is changed.



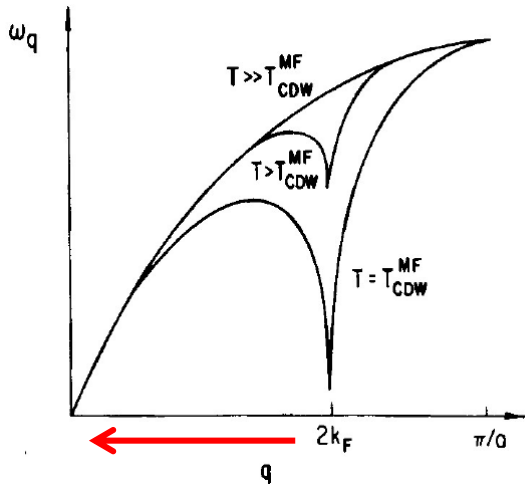
Acoustic phonon for LSMO



**To our knowledge, such low energy scales of CDW amplitude modes (0.1 THz, 0.3 THz) were not seen/reported in any other CDW materials.**

The low energy scale of amplitude mode ( $\sim 4 \text{ cm}^{-1}$ ) is hard to be detected by other techniques (e.g. Raman).

# What is the reason behind?



One possible scenario:

Because of the very small nesting wave vector  $2k_F$ , the acoustic phonon mode, which experiences a softening to zero frequency and triggers the CDW transition, also has very low energy scale.

$$\omega_{2k_F} \approx v_{\text{phonon}} \cdot 2k_F$$

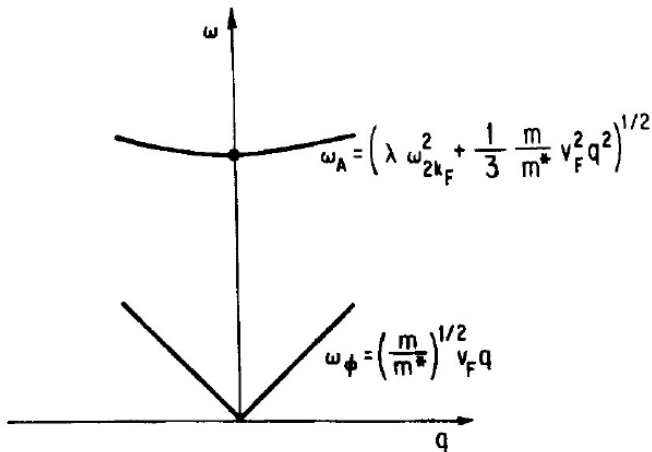
At  $q=0$ , the amplitude mode energy

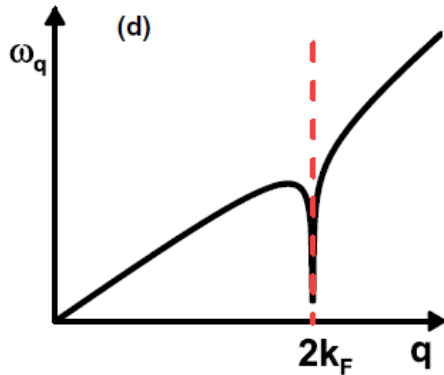
$$\omega_A = \omega_{2k_F} \cdot \lambda^{1/2}$$



very low energy scale of  $\omega_A$

It also explain why the lower CDW order has higher amplitude mode energy, because of bigger nesting wave vector.





Information about velocities of  $V_{F1}$  and  $V_{F2}$  two acoustic phonon branches which experience softening:

$$\frac{V_{F1}}{V_{F2}} = \frac{\omega_{2k_{F1}}/2k_{F1}}{\omega_{2k_{F2}}/2k_{F2}} \sim \frac{\nu_1/k_{F1}}{\nu_2/k_{F2}} \sim 2.2$$

The in-plane one has higher velocity (about two times higher).



# Conclusion

- We clearly observe the energy gap formation below the CDW phase transition temperatures in optical conductivity.
- We observe two **CDW amplitude modes with extremely low energy scales.**
- The amplitude and relaxation time of the transient reflectivity remains unchanged across the two phase transitions
- Those unusual properties are closely linked to the extremely small nesting wave vectors of the two CDW orders.
- Possible effect of AM on low energy physical properties?

Thank you !

# K0.3MoO3

